

Article

Improved Sliding Mode Finite-Time Synchronization of Chaotic Systems with Unknown Parameters

Hao Jia ^{1,2,*}, Chen Guo ¹, Lina Zhao ² and Zhao Xu ²

¹ College of Marine Electrical Engineering, Dalian Maritime University, Dalian 116026, China; guoc@dmlu.edu.cn

² School of Electrical Engineering, Dalian University of Science and Technology, Dalian 116052, China; zln0225@outlook.com (L.Z.); ffxzy@dlust.edu.cn (Z.X.)

* Correspondence: haun_jia@dmlu.edu.cn; Tel.: +86-0411-8624-5060

Received: 18 November 2020; Accepted: 17 December 2020; Published: 20 December 2020



Abstract: This work uses the sliding mode control method to conduct the finite-time synchronization of chaotic systems. The utilized parameter selection principle differs from conventional methods. The designed controller selects the unknown parameters independently from the system model. These parameters enable tracking and prediction of the additional variables that affect the chaotic motion but are difficult to measure. Consequently, the proposed approach avoids the limitations of selecting the unknown parameters that are challenging to measure or modeling the parameters solely within the relevant system. This paper proposes a novel nonsingular terminal sliding surface and demonstrates its finite-time convergence. Then, the adaptive law of unknown parameters is presented. Next, the adaptive sliding mode controller based on the finite-time control idea is proposed, and its finite-time convergence and stability are discussed. Finally, the paper presents numerical simulations of chaotic systems with either the same or different structures, thus verifying the proposed method's applicability and effectiveness.

Keywords: chaotic synchronization; finite-time control; nonsingular terminal sliding mode surface; unknown parameter selection

1. Introduction

The chaos system is a special kind of nonlinear system, and chaos will occur in many aspects. The chaos phenomenon is generally caused by disturbances and the system parameters satisfying certain conditions. Thus, to improve the operation reliability of the system, sometimes this chaos phenomenon should be avoided. Discussions on the relation between the chaos and bifurcation phenomenon, and the non-linear oscillation of the system are very popular. Most scholars study how to ensure the stable operation of the system. This research is also of significance for the above-mentioned chaos control of one class of system in practice.

In most cases, the control of chaotic system refers to the synchronization control of the system. Therefore, in recent years, chaotic system synchronization control has attracted significant attention within the fields of mathematics, physics and, engineering science. The research findings on chaotic system synchronization are widely applied in securing communication, power conversion, biological systems, information processing, and chemical reactions [1]. The primary approach to two chaotic systems' synchronization relies on designing an appropriate controller that controls the slave system, making the slave system state asymptotically track the main system state.

Numerous control techniques (e.g., in differential dynamics and bifurcation theory) of chaotic systems synchronization have emerged [2]. Specific methods include classical Proportional–Integral–Derivative (PID) control [3], adaptive fuzzy control, adaptive pulse

perturbation [4], random Melnikov method [5], negative feedback algorithm [6], and chaotic synchronization based on the ant colony algorithm [7]. Alzarano et al. [8] used the Melnikov method to study the bifurcation phenomenon of chaotic motion, while Bikdashetal [9] utilized it in researching the fractal state of rolling chaotic motion. Path tracking technique was used in [10], where the authors found a nonlinear bifurcation set with six degrees of freedom and obtained the chaotic attractors generated by periodical system multiplication. Acanfora et al. [11] used the optimization algorithm to explain the phase spectrum's influence on resonance phenomenon development, given the mixed nonlinear model of six degrees of freedom.

In early research works, the chaotic system's parameters were commonly assumed to be known in advance. However, in the majority of real-world systems, external natural factors inevitably disturb the chaotic system parameters, thus changing the parameter values. Consequently, the synchronization of chaotic systems' unknown parameters has become an important research direction in recent years. The chaotic systems unknown parameters' synchronization methods include a sliding mode control [12,13], backstepping design [14], optimum control [15], adaptive control [16], linear balanced feedback control [17], active control [18], pulse control, and fuzzy control [19]. In most cases, the parameters inside the system model are directly selected as unknown parameters, which has certain limitations, because of the parameters outside the system model cannot be identified. The listed studies on the synchronization of unknown parameters in chaotic systems pose no time requirements and guarantee asymptotic stability. In other words, the time approaches infinity until the system synchronization is achieved. However, practical applications require achieving system synchronization within finite time. In addition, the finite-time control approaches were shown to result in better robustness and anti-interference performance. Several researchers realized the chaotic synchronization control using the finite-time control techniques, such as finite-time stochastic method [20], CLF-based method [21], sliding mode control [22], and pure finite-time control method [23].

As mentioned above, the unknown parameters of a chaotic system are usually selected in a system model. For example, in works such as [24,25], relevant model parameters are directly set and regarded as unknown. Since system models contain multiple parameters, careful analysis and argumentation are needed when choosing the unknown parameters. Additionally, in general, several parameters cannot be regarded as unknown.

Building on the presented discussion, this paper proposes a novel finite-time control method for chaotic systems with unknown parameters. The control strategy is based on sliding mode control technology. The controller is model-based, but the controller unknown parameter adaptation only depends on the sliding surface instead of directly selecting the relevant unknown parameters in the system model, and the sliding surface has new forms. In this way, the selected parameters might be the outside unknown variables of the system model that affect chaotic motion, which are challenging to measure. The proposed approach avoids the difficulties of the unknown parameters selection and mitigates the limitations of choosing the relevant parameters within the system model only. The paper demonstrates the proposed method's finite-time convergence. The adaptive law of unknown parameters is then presented to make the synchronization error system reach the sliding mode surface in finite-time. Simultaneously, simulation verification is conducted using chaotic systems with the same, as well as different, structures. The results show a good control effect. This paper discusses the mathematical theory enabling the realization of the proposed approach. However, further analysis is required to determine the specific parameters' value for different chaotic phenomena applications.

The rest of the paper is structured as follows. Section 1 presents the fundamental lemmas used in the research. In Section 2, a new sliding surface is proposed for a general nonlinear chaotic system. Additionally, the sliding mode controller that deals with unknown parameters independent of the controlled system model is designed within this section. The adaptive law of unknown parameters is described, and the finite-time stability is proved. In Section 3, simulation verification is performed, demonstrating the same-structure synchronization of the parametric excitation rolling chaotic system

of a ship, as well as the different structures' synchronization of the Liu system and the Lorenz system. Section 4 concludes the paper and discusses the directions for further research.

2. Fundamental Lemmas

In this section, the system description is presented, the synchronization problem is explained, and the relevant definitions and several necessary lemmas on finite-time synchronization are introduced.

The following two n -dimensional chaotic systems are considered:

Master system:

$$\begin{cases} \dot{x}_1(t) = f_1(x_1, x_2, \dots, x_n) \\ \dot{x}_2(t) = f_2(x_1, x_2, \dots, x_n) \\ \vdots \\ \dot{x}_n(t) = f_n(x_1, x_2, \dots, x_n) \end{cases}, \tag{1}$$

Slave system:

$$\begin{cases} \dot{y}_1(t) = g_1(y_1, y_2, \dots, y_n) + u_1(t) \\ \dot{y}_2(t) = g_2(y_1, y_2, \dots, y_n) + u_2(t) \\ \vdots \\ \dot{y}_n(t) = g_n(y_1, y_2, \dots, y_n) + u_n(t) \end{cases}. \tag{2}$$

In the above equation, $f_i(x_1, x_2, \dots, x_n), i = 1, 2, \dots, n$ and $g_i(y_1, y_2, \dots, y_n), i = 1, 2, \dots, n$ are nonlinear functions, and $u_i(t), i = 1, 2, \dots, n$ is a controller with unknown parameters. Equations (1) and (2) both represent chaotic systems.

This work aims at designing a suitable controller with particular unknown parameters independent of the system model to synchronize chaotic systems (described by Equations (1) and (2)) in a finite time while the systems remain chaotic. To achieve finite-time synchronization, a system error is defined as follows:

$$e_i(t) = x_i(t) - y_i(t), \tag{3}$$

The error dynamics equation is obtained as a derivative of the equation resulting from subtracting Equation (3) from Equation (2). Thus:

$$\begin{cases} \dot{e}_1(t) = f_1(x_i) - g_1(y_i) - u_1(t) \\ \dot{e}_2(t) = f_2(x_i) - g_2(y_i) - u_2(t) \\ \vdots \\ \dot{e}_i(t) = f_i(x_i) - g_i(y_i) - u_i(t) \\ \vdots \\ \dot{e}_n(t) = f_n(x_i) - g_n(y_i) - u_n(t) \end{cases}. \tag{4}$$

Definition 1. Let the master system be defined with Equation (1) and the slave system with Equation (2). Suppose there is a constant $T > 0$ for which $\lim_{t \rightarrow T} |e_i(t)| = 0, i = 1, 2, \dots, n$ and $|e_i(t)| \equiv 0, i = 1, 2, \dots, n$ when $t > T$. Then, the chaotic synchronization of systems (1) and (2) is achieved in finite time T .

Achieving the finite-time stabilization of the error system (4) is equivalent to realizing the finite-time synchronization of chaotic systems (1) and (2).

Lemma 1 [26]. Consider a system (5)

$$\dot{\mathbf{x}} = \mathbf{f}(\mathbf{x}), \mathbf{f}(0) = 0, \mathbf{x} \in R^n, \tag{5}$$

where $\mathbf{f} : D \rightarrow R^n$ is continuous on an open neighborhood and $D \subset R^n$. Assuming that there is a continuous differential positive-definite function $V(\mathbf{x}) : D \rightarrow R$, and the real numbers $p > 0$ and $0 < \eta < 1$ satisfy:

$$V(\mathbf{x}) + pV^\eta(\mathbf{x}) \leq 0, \forall \mathbf{x} \in D, \tag{6}$$

then, the system (5) is a finite-time stable system whose stabilization time depends on the initial state $\mathbf{x}(0) = \mathbf{x}_0$ (here $\mathbf{x}(0)$ represent vectors, for example $\mathbf{x} = (x_1, x_2 \dots x_i)$, so $\mathbf{x}(0) = \mathbf{x}_0 = (x_1(0), x_2(0) \dots x_i(0))$, the initial conditions are simple initial conditions) and satisfies:

$$T(\mathbf{x}_0) \leq \frac{V^{1-\eta}(\mathbf{x}_0)}{p(1-\eta)}. \tag{7}$$

Note 1. Throughout the paper, symbols written in boldface represent vectors.

Lemma 2 [27]. For every $a_1, a_2, \dots, a_n \in R$, the following equation is satisfied:

$$|a_1| + |a_2| + \dots + |a_n| \geq \sqrt{a_1^2 + a_2^2 + \dots + a_n^2}. \tag{8}$$

3. Design of Sliding Mode Surface and Controller

This section introduces a new sliding mode controller that realizes the chaotic synchronization of two different chaotic systems in a finite time. In doing so, the two main procedures include designing a sliding surface and guaranteeing the finite-time stability of the system on a sliding surface. First, an adaptive finite-time controller with unknown parameters independent of the system model is designed. Then, convergence to sliding surface within finite time is guaranteed, and the adaptive law of unknown parameters is designed.

The designed novel sliding surface is:

$$s_i(t) = c_i e_i(t) + \int_0^t \text{sgn}(e_i(\tau)) |e_i(\tau)|^\alpha d\tau + e_i(t) \text{sgn}(e_i(t)), i = 1, 2, \dots, n, \tag{9}$$

where $s_i(t) \in R$, and c_i and α are constants for which $c_i > 0$ and $0 < \alpha < 1$. Taking the first-order derivative of the sliding surface, one obtains:

$$\dot{s}_i(t) = c_i \dot{e}_i(t) + \text{sgn}(e_i(t)) |e_i(t)|^\alpha + \dot{e}_i(t) \text{sgn}(e_i(t)), i = 1, 2, \dots, n. \tag{10}$$

Based on the sliding mode control principle [28],

$$\dot{e}_i(t) = -\frac{\text{sgn}(e_i(t))}{c_i + \text{sgn}(e_i(t))} |e_i(t)|^\alpha. \tag{11}$$

Let

$$c_i + \text{sgn}(e_i(t)) = d_i > 0,$$

Then

$$\dot{s}_i(t) = d_i \dot{e}_i(t) + \text{sgn}(e_i(t)) |e_i(t)|^\alpha, i = 1, 2, \dots, n, \tag{12}$$

$$\dot{e}_i(t) = -\frac{\text{sgn}(e_i(t))}{d_i} |e_i(t)|^\alpha. \tag{13}$$

Theorem 1. Consider the error dynamics Equation (13). Under the introduced sliding surface, the system is finite-time stable, and the time T_1 required to reach the equilibrium $e_i(t) = 0$ is determined by:

$$T_1 \leq \frac{(1/2 \sum_{i=1}^n e_i^2(0))^{\frac{1-\alpha}{2}}}{(1-\alpha)\rho 2^{\frac{1-\alpha}{2}}}, \tag{14}$$

where ρ is the minimum value among $\frac{1}{d_i}, \forall i = 1, 2, \dots, n$.

Proof of Theorem 1. Consider the Lyapunov function: $V(t) = \frac{1}{2} \sum_{i=1}^n e_i^2(t)$.

The function's first-order derivative relative to time equals: $\dot{V}(t) = \sum_{i=1}^n e_i(t) \dot{e}_i(t)$.

Then, using (13), one obtains: $\dot{V}(t) = \sum_{i=1}^n e_i(t) (-\frac{1}{d_i} \text{sgn}(e_i(t)) |e_i(t)|^\alpha)$,

$$\dot{V}(t) = -\sum_{i=1}^n \frac{1}{d_i} |e_i(t)|^{\alpha+1} \leq -\rho \sum_{i=1}^n |e_i(t)|^{\alpha+1},$$

Utilizing Lemma 2, it follows: $\dot{V}(t) \leq -\rho \sum_{i=1}^n |e_i(t)|^{\alpha+1} \leq -2^{\frac{\alpha+1}{2}} \rho (\frac{1}{2} \sum_{i=1}^n e_i^2(t))^{\frac{\alpha+1}{2}} = -2^{\frac{\alpha+1}{2}} \rho V^{\frac{\alpha+1}{2}}(t)$.

Therefore, $\dot{V}(t) + 2^{\frac{\alpha+1}{2}} \rho V^{\frac{\alpha+1}{2}}(t) \leq 0$, where $2^{\frac{\alpha+1}{2}} \rho > 0$ and $0 < \frac{\alpha+1}{2} < 1$. Since Equation (6) is satisfied, following the Lemma 1 one obtains: $T_1 \leq \frac{(1/2 \sum_{i=1}^n e_i^2(0))^{\frac{1-\alpha}{2}}}{(1-\alpha)\rho 2^{\frac{1-\alpha}{2}}}$.

Hence, the error $e_i(t), i = 1, 2, \dots, n$ converges to zero in finite time T_1 . In other words, systems (1) and (2) synchronize in a finite time. The proof is finished. \square

Once the sliding surface is designed, one needs to design a controller with unknown parameters independent of the system model and ensure the error system converges to the sliding surface within finite time. Therefore, the existence of a sliding surface, as well as the convergence of the error trajectory $e_i(t), i = 1, 2, \dots, n$ to sliding surface $s_i(t) = 0, i = 1, 2, \dots, n$ should be guaranteed. Then, Systems (1) and (2) reach chaotic synchronization.

The designed controller is as follows:

$$u_i(t) = f_i(x_i) - g_i(y_i) + \frac{1}{d_i} [\text{sgn}(e_i(t)) |e_i(t)|^\alpha + \hat{k}_i \frac{|s_i(t)|}{s_i(t)}], \tag{15}$$

where $i = 1, 2, \dots, n, d_i = c_i + \text{sgn}(e_i(t)) > 0$, and $k_i > 0$. Here k_i denotes the unknown parameters that are greater than zero and independent of the synchronized system model. Symbol \hat{k}_i denotes the estimated value of unknown parameter k_i . Note that the unknown parameter k_i is not within the system model (1) and only depends on the sliding surface. For the conventional approach, the unknown parameters are selected in the

system model (e.g., [22] and [23]). Therefore, these parameters can be seen as the arbitrary factors that affect the system and are difficult to predict or measure. The adaptive law of unknown parameter k_i is defined as:

$$\dot{\hat{k}}_i = |s_i(t)| - k_i \frac{|\hat{k}_i - k_i|}{(\hat{k}_i - k_i)}. \tag{16}$$

The control law proposed in Equation (15) and the adaptive law in Equation (16) ensure the sliding motion occurs in a finite time. The following theorem demonstrates such a claim.

Theorem 2. When the control law (15) and the adaptive law (16) are used to control the error system (4), the system state moves towards the sliding surface and approaches the sliding surface $s_i(t) = 0, i = 1, 2, \dots, n$ in a finite time, denoted T_2 . Time T_2 is determined by:

$$T_2 \leq \frac{(\frac{1}{2} \sum_{i=1}^n [s_i(0)]^2 + \frac{1}{2} \sum_{i=1}^n \tilde{k}_i^2(0))^{\frac{1}{2}}}{2^{-\frac{1}{2}} \rho} \tag{17}$$

where \tilde{k}_i denotes the errors of unknown parameters ($\tilde{k}_i = \hat{k}_i - k_i, \forall i = 1, 2, \dots, n$).

Proof of Theorem 2. Consider the Lyapunov function: $V(t) = \frac{1}{2} \sum_{i=1}^n [s_i(t)]^2 + \frac{1}{2} \sum_{i=1}^n \tilde{k}_i^2$, where \tilde{k}_i is the error of unknown parameter. Clearly, $\dot{\tilde{k}}_i = \dot{\hat{k}}_i$. Calculating the first-order derivative of $V(t)$, one obtains:

$$\dot{V}(t) = \sum_{i=1}^n [s_i(t) \dot{s}_i(t)] + \sum_{i=1}^n [\tilde{k}_i \dot{\tilde{k}}_i].$$

Utilizing Equation (12), it follows: $\dot{V}(t) = \sum_{i=1}^n [s_i(t)(d_i e_i(t) + \text{sgn}(e_i(t))|e_i(t)|^\alpha)] + \sum_{i=1}^n [\tilde{k}_i \dot{\tilde{k}}_i]$.

Next, using Equation (4), one derives:

$$\dot{V}(t) = \sum_{i=1}^n [s_i(t)(d_i(f_i(x_i) - g_i(y_i) - u_i(t)) + \text{sgn}(e_i(t))|e_i(t)|^\alpha)] + \sum_{i=1}^n [\tilde{k}_i \dot{\tilde{k}}_i].$$

Then, one can utilize Equation (15) to obtain:

$$\begin{aligned} \dot{V}(t) &= \sum_{i=1}^n [s_i(t)(d_i(f_i(x_i) - g_i(y_i) - (f_i(x_i) - g_i(y_i) + \\ &\frac{1}{d_i}[\text{sgn}(e_i(t))|e_i(t)|^\alpha + \hat{k}_i \frac{|s_i(t)|}{s_i(t})])) + \text{sgn}(e_i(t))|e_i(t)|^\alpha)] + \sum_{i=1}^n [\tilde{k}_i \dot{\tilde{k}}_i] \\ &= - \sum_{i=1}^n [s_i(t)(\hat{k}_i \frac{|s_i(t)|}{s_i(t)})] + \sum_{i=1}^n [\tilde{k}_i \dot{\tilde{k}}_i] \\ &= - \sum_{i=1}^n [\hat{k}_i |s_i(t)|] + \sum_{i=1}^n [\tilde{k}_i \dot{\tilde{k}}_i] \\ &= - \sum_{i=1}^n [\hat{k}_i |s_i(t)|] + \sum_{i=1}^n [\hat{k}_i - k_i] \dot{\hat{k}}_i \end{aligned}$$

From Equation (16) follows:

$$\begin{aligned} \dot{V}(t) &= - \sum_{i=1}^n [\hat{k}_i |s_i(t)|] + \sum_{i=1}^n [(\hat{k}_i - k_i) \dot{\hat{k}}_i] = - \sum_{i=1}^n [\hat{k}_i |s_i(t)|] + \sum_{i=1}^n [(\hat{k}_i - k_i) [|s_i(t)| - k_i \frac{|\hat{k}_i - k_i|}{(\hat{k}_i - k_i)}]] \\ &= - \sum_{i=1}^n [k_i |s_i(t)|] - \sum_{i=1}^n k_i |\hat{k}_i - k_i| \end{aligned}$$

Thus,

$$\dot{V}(t) = -\sum_{i=1}^n [k_i |s_i(t)|] - \sum_{i=1}^n k_i |\hat{k}_i - k_i| \leq -\gamma \left(\sum_{i=1}^n [|s_i(t)|] + \sum_{i=1}^n [|\hat{k}_i - k_i|] \right).$$

where γ denotes the minimum value among k_i . Using Equation (8) in Lemma 2, it follows:

$$\begin{aligned} -\gamma \left(\sum_{i=1}^n [|s_i(t)|] + \sum_{i=1}^n [|\hat{k}_i - k_i|] \right) &\leq -\gamma \left(\sum_{i=1}^n [s_i(t)]^2 + \sum_{i=1}^n \tilde{k}_i^2 \right)^{\frac{1}{2}} = -2^{\frac{1}{2}} \gamma \left(\frac{1}{2} \sum_{i=1}^n [s_i(t)]^2 + \frac{1}{2} \sum_{i=1}^n \tilde{k}_i^2 \right)^{\frac{1}{2}} \\ &= -2^{\frac{1}{2}} \gamma V^{\frac{1}{2}}(t) \leq 0 \end{aligned}$$

where $2^{\frac{1}{2}} \gamma > 0, 0 < \frac{1}{2} < 1$. Since Equation (6) is satisfied, Lemma 1 gives:

$$T_2 \leq \frac{\left(\frac{1}{2} \sum_{i=1}^n [s_i(0)]^2 + \frac{1}{2} \sum_{i=1}^n \tilde{k}_i^2(0) \right)^{\frac{1}{2}}}{2^{-\frac{1}{2}} \gamma}.$$

Therefore, the error trajectory $e_i(t)$ converges to sliding mode surface $s_i(t) = 0$ in finite time T_2 . The proof is finished. \square

In summary, the block diagram of synchronization and control scheme is as follows:

Note 2. Following Theorems 1 and 2, the sliding mode controller (15) with the adaptive law (16) and sliding surface (9) enables synchronization of systems (1) and (2) within finite time. The synchronization time equals $T = T_1 + T_2$.

Note 3. Constant c_i is directly proportional to convergence times T_1 and T_2 . Thus, a smaller c_i results in shorter T_1 and T_2 . On the other hand, from Equation (15), it follows that the controller input $u_i(t)$ is inversely proportional to c_i , meaning that smaller c_i leads to greater $u_i(t)$.

4. Simulation Verification

In this section, MATLAB software is used to perform numerical simulations of chaotic systems with either the same or with different structures [29,30]. The chaotic systems' synchronization is realized utilizing the novel sliding surface and controller designed in the previous section. Additionally, the introduction of unknown parameters independent of the system model is realized, and the adaptive law is presented.

4.1. Simulation Verification of Parametric Excitation Rolling Chaotic System of Ship with the Same Structure

The nonlinear mathematical model for the roll system of a ship with parametric and forced excitation in a regular longitudinal wave is as follows:

$$\ddot{\phi} + \mu_1 \dot{\phi} + \mu_3 \phi^3 + \omega_0^2 (\phi + \alpha_3 \phi^3 + \alpha_5 \phi^5 + h_0 \phi \cos(\omega_1 t)) = K_e \sin(\omega_1 t + \delta_0),$$

where $\phi(t)$ is the roll angle; h_0 is the amplitude of parametric excitation; ω_1 is the frequency of metric excitation, which is usually twice that of the natural frequency when chaos occurs in the system; μ_1 and μ_3 are the damping factors of the roll; α_3 and α_5 are the dimensionless righting moment coefficients; ω_0 is the natural frequency of the ship roll; and $K_e \sin(\omega_1 t + \delta_0)$ is the forced roll moment in regular waves, where K_e is the amplitude of the forced excitation and δ_0 is encounter location of the ship and regular wave, assigned as 0.

After the above parameters are determined, the nonlinear mathematical model for the roll system of a ship with parametric and forced excitation is changed to the following:

$$\ddot{\phi} + 0.069\dot{\phi} + 0.5367\phi^3 + 1.25\phi - 0.9926\phi^3 + 0.0998\phi^5 + 2.875\phi \cos 2.236t = 0.16 \sin 2.236t$$

Let $x_1(t) = \phi(t), x_2(t) = \dot{\phi}(t)$, and, by conversion to state equations, it is obtained as follows:

$$\begin{cases} \dot{x}_1 = x_2 \\ \dot{x}_2 = -0.069x_2 - 0.5367x_2^3 - 1.25x_1 + 0.9926x_1^3 - 0.0998x_1^5 - 2.875x_1 \cos 2.236t + 0.16 \sin 2.236t \end{cases} \quad (18)$$

The parametric excitation roll system of a ship is a chaos system that can be proved by MATLAB simulation results. The history charts of x_1 and x_2 of the parametric excitation roll system of the ship are shown in Figures 1 and 2, respectively, in which it is clear that the system is in chaos. The phase diagram of the parametric excitation roll system of the ship is shown in Figure 3, which further proves that the system is a chaos system and similar to a Duffing chaos system.

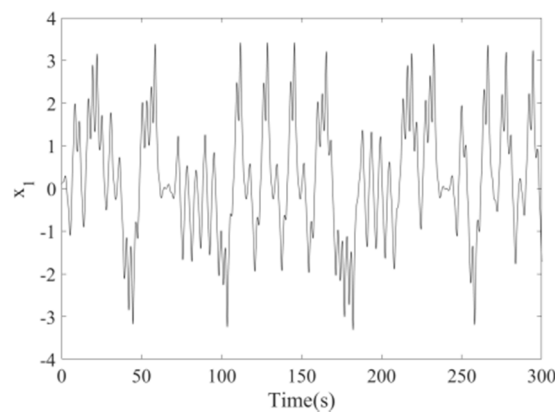


Figure 1. The time response of x_1 about ship parametric excitation rolling system Equation (18).

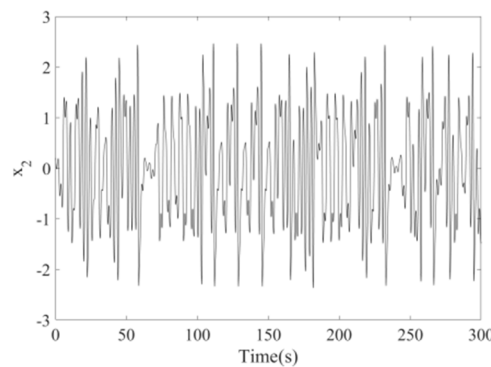


Figure 2. The time response of x_2 about ship parametric excitation rolling system Equation (18).

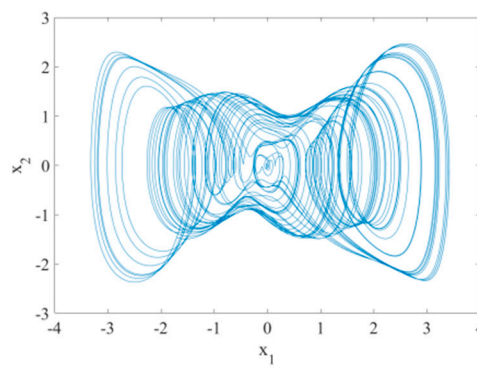


Figure 3. The phase diagram of x_1 and x_2 about ship parametric excitation rolling system.

In the traditional methods, h_0 and ω_1 are usually chosen as unknown parameters. In the model $\ddot{\phi} + \mu_1\dot{\phi} + \mu_3\phi^3 + \omega_0^2(\phi + \alpha_3\phi^3 + \alpha_5\phi^5 + h_0\phi \cos(\omega_1 t)) = K_e \sin(\omega_1 t + \delta_0)$, h_0 is parameter excitation amplitude and ω_1 is parameter excitation frequency, which can affect the chaotic state of the system. This method can be seen in references [24] and [25].

In the method discussed in this paper, a ship’s parametric excitation rolling system is regarded as a master system. The controller’s chaotic system with unknown parameters independent of the system model is regarded as a slave system. The master system and slave system are based on the ship parametric excitation rolling system with the same fundamental structure. In other words, the chaotic control is achieved over the same structure systems.

Master system:

$$\begin{cases} \dot{x}_1 = x_2 \\ \dot{x}_2 = -0.069x_2 - 0.5367x_2^3 - 1.25x_1 + 0.9926x_1^3 - 0.0998x_1^5 \\ -2.875x_1 \cos 2.236t + 0.16 \sin 2.236t \end{cases}, \tag{19}$$

Slave system:

$$\begin{cases} \dot{y}_1 = y_2 + u_1(t) \\ \dot{y}_2 = -0.069y_2 - 0.5367y_2^3 - 1.25y_1 + 0.9926y_1^3 - 0.0998y_1^5 \\ -2.875y_1 \cos 2.236t + 0.16 \sin 2.236t + u_2(t) \end{cases}, \tag{20}$$

$$\text{Error system : } \begin{cases} e_1 = x_1 - y_1 \\ e_2 = x_2 - y_2 \end{cases},$$

Error dynamics equation:

$$\begin{cases} \dot{e}_1 = x_2 - y_2 - u_1(t) \\ \dot{e}_2 = -0.069x_2 - 0.5367x_2^3 - 1.25x_1 + 0.9926x_1^3 - 0.0998x_1^5 \\ -2.875x_1 \cos 2.236t + 0.16 \sin 2.236t + 0.069y_2 + \\ 0.5367y_2^3 + 1.25y_1 - 0.9926y_1^3 + 0.0998y_1^5 \\ +2.875y_1 \cos 2.236t - 0.16 \sin 2.236t - u_2(t) \end{cases}, \tag{21}$$

Using Equation (9), the sliding mode surface is designed as follows:

$$\begin{cases} s_1 = c_1 e_1(t) + \int_0^t \text{sgn}(e_1(\tau)) |e_1(\tau)|^\alpha d\tau + e_1(t) \text{sgn}(e_1(t)) \\ s_2 = c_2 e_2(t) + \int_0^t \text{sgn}(e_2(\tau)) |e_2(\tau)|^\alpha d\tau + e_2(t) \text{sgn}(e_2(t)) \end{cases}, \tag{22}$$

According to Equation (15), the controller with unknown parameters independent of the system is designed as:

$$\begin{cases} u_1(t) = x_2 - y_2 + \frac{1}{c_1 + \text{sgn}(e_1(t))} [\text{sgn}(e_1(\tau)) |e_1(\tau)|^\alpha + \hat{k}_1 \frac{|s_1|}{s_1}] \\ u_2(t) = -0.069x_2 - 0.5367x_2^3 - 1.25x_1 + 0.9926x_1^3 - 0.0998x_1^5 \\ -2.875x_1 \cos 2.236t + 0.16 \sin 2.236t + 0.069y_2 + 0.5367y_2^3 \\ + 1.25y_1 - 0.9926y_1^3 + 0.0998y_1^5 + 2.875y_1 \cos 2.236t \\ -0.16 \sin 2.236t + \frac{1}{c_2 + \text{sgn}(e_2(t))} [\text{sgn}(e_2(\tau)) |e_2(\tau)|^\alpha + \hat{k}_2 \frac{|s_2|}{s_2}] \end{cases}, \quad (23)$$

From Equation (16), the adaptive law of unknown parameters is:

$$\begin{cases} \dot{\hat{k}}_1 = |s_1| - k_1 \frac{|\hat{k}_1 - k_1|}{(\hat{k}_1 - k_1)} \\ \dot{\hat{k}}_2 = |s_2| - k_2 \frac{|\hat{k}_2 - k_2|}{(\hat{k}_2 - k_2)} \end{cases}. \quad (24)$$

In the simulation, the step size was set to 0.01 s, and the initial values were $x_1(0) = 3, x_2(0) = 3, y_1(0) = 1, y_2(0) = 1$, and $c_1 = 8, c_2 = 9$. In addition, the initial values of unknown parameters were set to $k_1 = 0.1$ and $k_2 = 0.2$.

Figures 4 and 5 reflect the synchronization process of Systems (19) and (20), and synchronization error is shown in Figure 6, the identification processes of unknown parameters k_1 and k_2 are shown in Figure 7. Figures 4 and 5 demonstrate that, when t approaches 2 s, the drive system parameters (x_1 and y_1) synchronize with the response system parameters (x_2 and y_2). The error effect in Figure 6 shows that, when t approaches 2 s, errors e_1 and e_2 stabilize around zero. Finally, Figure 7 demonstrates that, when t approaches 2 s, the parameters k_1 and k_2 reach values 6 and 7, respectively.

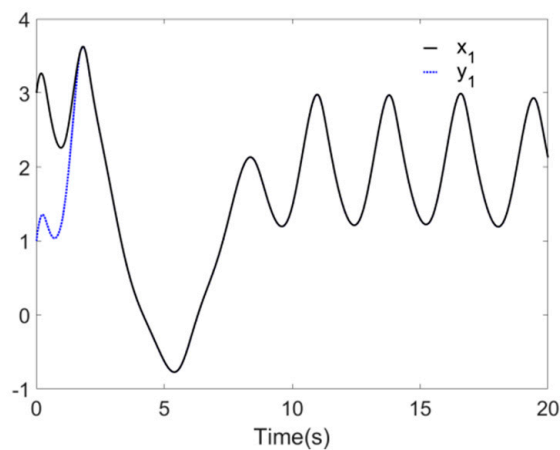


Figure 4. Synchronization process of y_1 arrives x_1 .

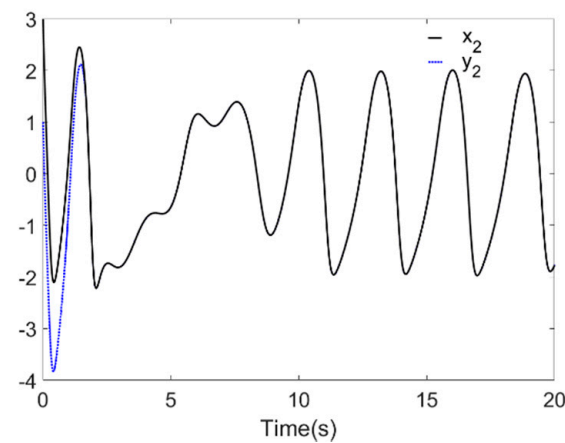


Figure 5. Synchronization process of y_2 arrives x_2 .

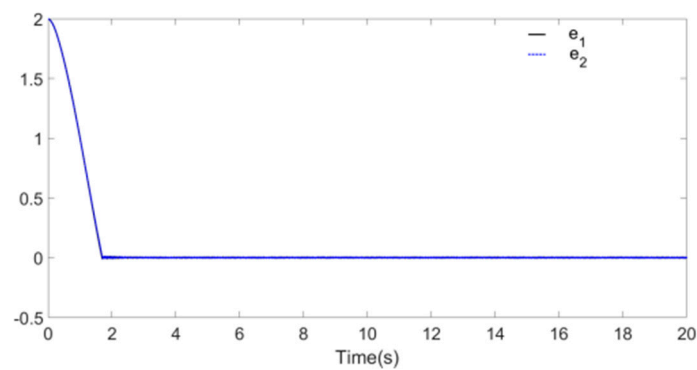


Figure 6. Synchronization errors.

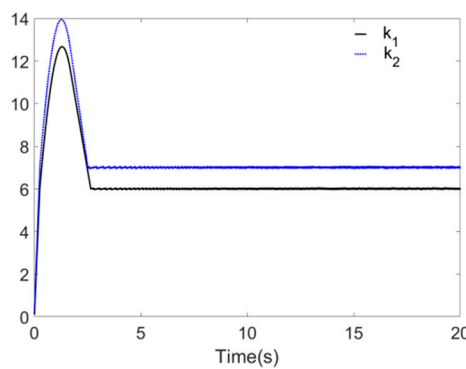


Figure 7. Identification process of k_1 and k_2 .

By using the parameters to update the rule (24), one can identify the special unknown parameters in the controller (23). In other words, the drive system and the response system reach a finite-time synchronization. After the controller facilitates the ship parametric excitation rolling system with unknown parameters independent of the system model, the response system successfully tracks the original system in a finite time. The adaptive parameters converge to bounded values within the finite time.

4.2. Simulation Verification of Chaotic System with Different Structures

Both the Liu system and the Lorenz system [31,32] are well-known chaotic systems that do not require a detailed introduction. In addition, their structures are different. In the traditional methods, the coefficients of the equations are usually chosen as unknown parameters. The coefficients of

these equations can affect the chaotic state of the system. This treatment method can be seen in references [24,25].

Here, the method mentioned in the previous section are used to verify the proposed method’s performance in the chaotic synchronization of systems with different structures.

Master system:

$$\text{Liu : } \begin{cases} \dot{x}_1 = -\frac{20}{7}x_1 - x_2x_3 + 10 \\ \dot{x}_2 = -10x_2 + x_1x_3 \\ \dot{x}_3 = -4x_3 + x_1x_2 \end{cases} , \tag{25}$$

Slave system:

$$\text{Lorenz : } \begin{cases} \dot{y}_1 = 10(y_2 - y_1) \\ \dot{y}_2 = 28y_1 - y_2 - y_1y_3 \\ \dot{y}_3 = y_1y_2 - \frac{8}{3}y_3 \end{cases} , \tag{26}$$

Using the Equation (9), the sliding mode surface is designed as follows:

$$\begin{cases} s_1 = c_1e_1(t) + \int_0^t \text{sgn}(e_1(\tau))|e_1(\tau)|^\alpha d\tau + e_1(t)\text{sgn}(e_1(t)) \\ s_2 = c_2e_2(t) + \int_0^t \text{sgn}(e_2(\tau))|e_2(\tau)|^\alpha d\tau + e_2(t)\text{sgn}(e_2(t)) \\ s_3 = c_3e_3(t) + \int_0^t \text{sgn}(e_3(\tau))|e_3(\tau)|^\alpha d\tau + e_3(t)\text{sgn}(e_3(t)) \end{cases} , \tag{27}$$

According to Equation (15), the controller with unknown parameters independent of the system is designed as:

$$\begin{cases} u_1(t) = 10(x_2 - x_1) - 10(y_2 - y_1) + \frac{1}{c_1 + \text{sgn}(e_1(t))} [\text{sgn}(e_1(\tau))|e_1(\tau)|^\alpha + \hat{k}_1 \frac{|s_1|}{s_1}] \\ u_2(t) = 40x_1 - x_1x_3 - (28y_1 - y_2 - y_1y_3) + \frac{1}{c_2 + \text{sgn}(e_2(t))} [\text{sgn}(e_2(\tau))|e_2(\tau)|^\alpha + \hat{k}_2 \frac{|s_2|}{s_2}] \\ u_3(t) = -2.5x_3 + 4x_1^2 - (y_1y_2 - \frac{8}{3}y_3) + \frac{1}{c_3 + \text{sgn}(e_3(t))} [\text{sgn}(e_3(\tau))|e_3(\tau)|^\alpha + \hat{k}_3 \frac{|s_3|}{s_3}] \end{cases} , \tag{28}$$

From Equation (16), the adaptive law of unknown parameters is:

$$\begin{cases} \dot{\hat{k}}_1 = |s_1| - k_1 \frac{|\hat{k}_1 - k_1|}{(\hat{k}_1 - k_1)} \\ \dot{\hat{k}}_2 = |s_2| - k_2 \frac{|\hat{k}_2 - k_2|}{(\hat{k}_2 - k_2)} \\ \dot{\hat{k}}_3 = |s_3| - k_3 \frac{|\hat{k}_3 - k_3|}{(\hat{k}_3 - k_3)} \end{cases} . \tag{29}$$

In the simulation, the step size was set to 0.01 s, and the initial values were $x_1(0) = -1.5, x_2(0) = 2.25, x_3(0) = 2.1, y_1(0) = 1, y_2(0) = 1, y_3(0) = 1$, and $c_1 = 8, c_2 = 9, c_3 = 10$. In addition, the initial values of unknown parameters were set to $k_1 = 0.1, k_2 = 0.2, k_3 = 0.3$.

Figures 8–10 reflect the synchronization process of Systems (25) and (26), and synchronization error is shown in Figure 11, the identification processes of unknown parameters k_1, k_2, k_3 are shown in Figure 12. Figures 8–10 demonstrate that, when t approaches 1.7 s, the drive system parameters (x_1, y_1 and z_1) synchronize with the response system parameters (x_2, y_2 and z_2). The error effect in Figure 11 shows that, when t approaches 1.7 s, errors e_1, e_2 , and e_3 stabilize around zero. Finally, Figure 12 demonstrates that, when t approaches 1.7 s, the parameters k_1, k_2 , and k_3 reach values 5.2, 2.5, and 2, respectively.

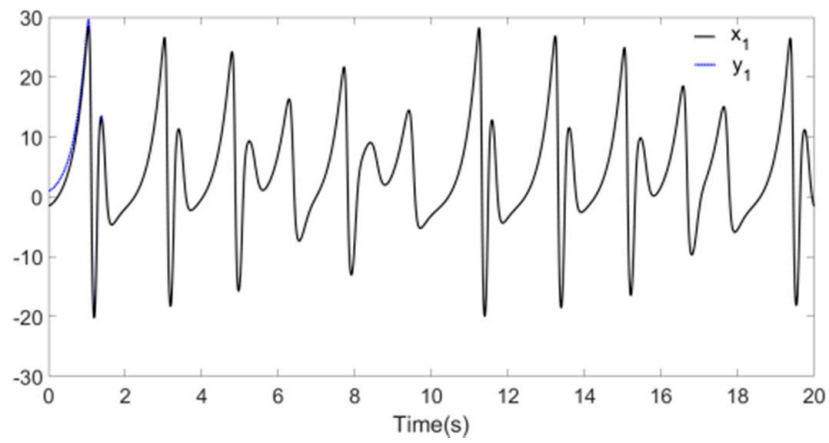


Figure 8. Synchronization of x_1 and y_1 .

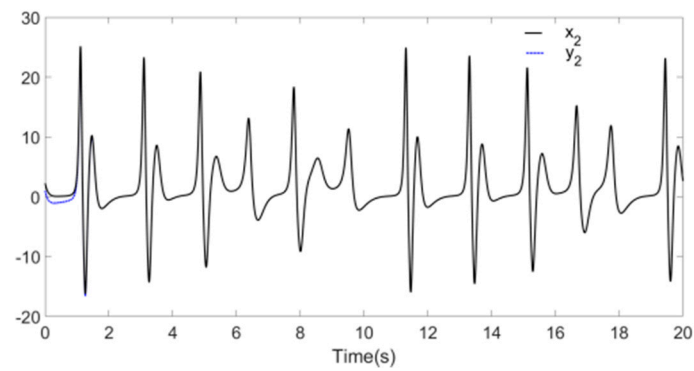


Figure 9. Synchronization of x_2 and y_2 .

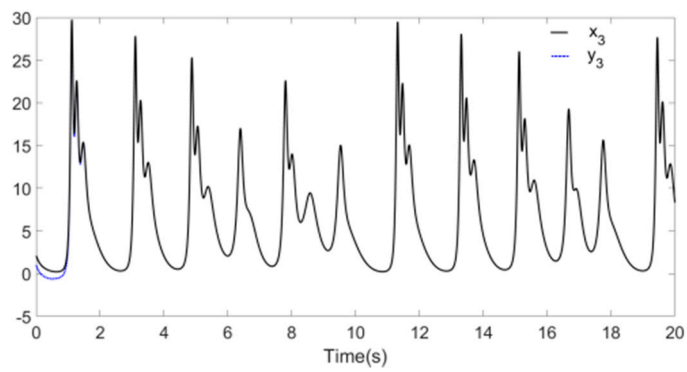


Figure 10. Synchronization of x_3 and y_3 .

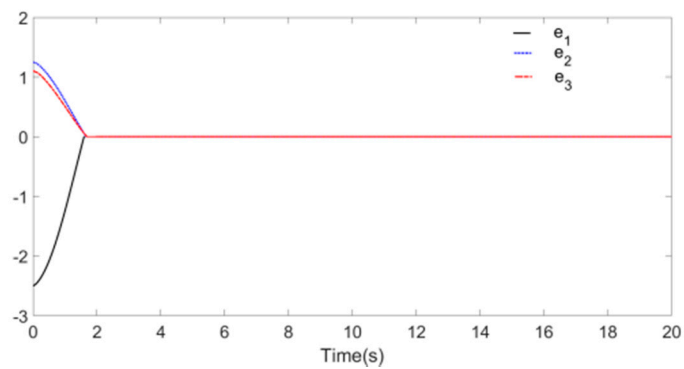


Figure 11. Synchronization error.

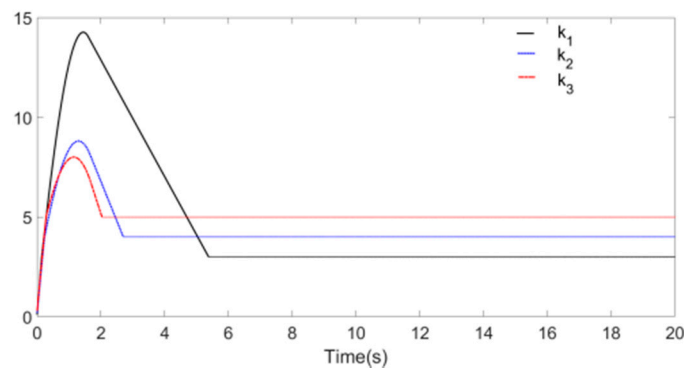


Figure 12. Identification process of k_1 , k_2 , and k_3 .

By using the parameters to update the rule (29), one can identify the special unknown parameters in the controller (28). In other words, the master system and the slave system reach a finite-time synchronization. The adaptive parameters converge to bounded values within the finite time. The effectiveness of the algorithm is further proved.

5. Conclusions

This paper uses a sliding mode control theory to study the finite-time synchronization problem of chaotic systems. A novel nonsingular terminal sliding surface was proposed. Additionally, a controller with unknown parameters only depends on the sliding surface, instead of directly selecting the relevant unknown parameters in the system model. The adaptive laws were designed, the convergence and the stability within finite time were proved. The simulation results demonstrate that synchronization of chaotic systems can be achieved in a finite time with high control speed, irrespective of whether the systems differ in structures or not. The practical meaning of the selected unknown parameters in specific chaotic systems will be further discussed in the subsequent studies.

Author Contributions: Conceptualization, C.G.; methodology, H.J.; software, H.J.; validation, L.Z.; formal analysis, Z.X.; resources, H.J.; data curation, L.Z.; writing—original draft preparation, L.Z.; writing—review and editing, Z.X.; supervision, C.G.; project administration, C.G.; funding acquisition, C.G. and Z.X. All authors have read and agreed to the published version of the manuscript.

Funding: This research was funded by the National Natural Science Foundation of China (grant numbers 51809028, 51579024, and 51879027) and the Scientific Research Funds project of the Education Department of Liaoning Province (grant number L2020009).

Acknowledgments: The data used to support the findings of this study are available from the corresponding author upon request.

Conflicts of Interest: The authors declare no conflict of interest.

References

- Liu, X.; Ma, L. Chaotic vibration, bifurcation, stabilization and synchronization control for fractional discrete-time systems. *Appl. Math. Comput.* **2020**, *385*, 125423. [[CrossRef](#)]
- Wang, L.; Peng, J.J. Yiming Synchronous Dynamics and Bifurcation Analysis in Two Delay Coupled Oscillators with Recurrent Inhibitory Loops. *J. Nonlinear Sci.* **2012**, *23*, 283–302. [[CrossRef](#)]
- Dong, E.; Chen, Z.; Yuan, Z. Control and synchronization of chaos systems based on neural network PID controller. *J. Jilin Univ.* **2007**, *37*, 646–650.
- Chen, Y.; Hwang, R.; Chang, C. Adaptive impulsive synchronization of uncertain chaotic systems. *Phys. Lett. A* **2010**, *374*, 2254–2258. [[CrossRef](#)]
- Li, S.; Wang, K. Chaos analysis of ship rolling motion in stochastic beam seas. *J. Ship Mech. Vibroengineering* **2017**, *19*, 6403–6412. [[CrossRef](#)]

6. Yao, Q.; Su, Y.; Li, L. Application of Negative Feedback Control Algorithm in Controlling Nonlinear Rolling Motion of Ships. In Proceedings of the 2018 7th International Conference on Advanced Materials and Computer Science (ICAMCS), Qingdao, China, 26–27 March 2016.
7. Wang, H.; Che, C.; Yu, L.; Liu, S.; You, J. Control method for a fin/tank integrated stabilization chaotic system. *CAAI Trans. Intell. Syst.* **2017**, *12*, 318–324.
8. Falzaranc, M.; Shaw, S.W.; Troesh, A.W. Application of global methods for analyzing dynamic systems to ships rolling motion and capsizing. *Int. J. Bifur. Chaos* **1992**, *2*, 101–115. [[CrossRef](#)]
9. Balachandran, B.B.; Nayfeh, A. Melnikov analysis for a ship with a general roll-damping model. *Nonlinear Dyn.* **1994**, *6*, 101–124.
10. Mulk, U.; Falzarano, J. Complete six degrees of freedom nonlinear ship rolling motion. *J. Offshore Mech. Arctic. Eng.* **1994**, *116*, 191–201. [[CrossRef](#)]
11. Acanfora, M.; Flavio, B.; Davide, L.; Enrico, R. A new identification method for non-linear roll resonance in irregular waves. *Ocean. Eng.* **2020**, *197*, 106809. [[CrossRef](#)]
12. Mohanty, N.P.; Dey, R.; Roy, B.K. Switching synchronisation of a 3-D multi-state-time-delay chaotic system including externally added memristor with hidden attractors and multi-scroll via sliding mode control. *Eur. Phys. J. Spec. Top.* **2020**, *229*, 1231–1244. [[CrossRef](#)]
13. Wang, J.; Liu, L.; Liu, C.; Li, X. Adaptive Sliding Mode Control Based on Equivalence Principle and Its Application to Chaos Control in a Seven-Dimensional Power System. *Math. Probl. Eng.* **2020**, *2020*, 1565460. [[CrossRef](#)]
14. El-Gohary, A. Optimal synchronization of Rössler system with complete uncertain parameters. *Chaos Solitons Fractals* **2006**, *27*, 345–355. [[CrossRef](#)]
15. Panaitescu, F.V.; Panaitescu, M.; Deleanu, D.; Anton, I.A. Analysis of environmental risk and extreme roll motions for a ship in waves. *J. Environ. Prot. Ecol.* **2019**, *20*, 1204–1213.
16. Chen, H.-H. Stability criterion for synchronization of chaotic systems using linear feedback control. *Phys. Lett. A* **2008**, *372*, 1841–1850. [[CrossRef](#)]
17. Jia, X.; Zhang, X. Application of Hoo controller to ship autopilot. *Control. Decis.* **1995**, *10*, 250–254.
18. Min, F.; Wang, Z. Generalized projective synchronization of two four-dimensional chaotic systems. *Ngon. Pqrstgn. Stutgn.* **2007**, *56*, 6238–6244.
19. Zhang, X.K. New method on design of robust controller for unstable process. In Proceedings of the International Conference on Machine Learning and Cybernetics, Lanzhou, China, 13–16 July 2014.
20. Yu, W. Finite-time stabilization of three-dimensional chaotic systems based on CLF. *Phys. Lett. A* **2010**, *374*, 3021–3024. [[CrossRef](#)]
21. Yang, X.; Cao, J. Finite-time stochastic synchronization of complex networks. *Appl. Math. Model.* **2010**, *34*, 3631–3641. [[CrossRef](#)]
22. Jianwen, F.; Ling, H.; Chen, X.; Austin, F.; Geng, W. Synchronizing the noise-perturbed Genesio chaotic system by sliding mode control. *Commun. Nonlinear Sci. Numer. Simul.* **2010**, *15*, 2546–2551. [[CrossRef](#)]
23. Wang, H.; Han, Z.; Xie, Q.; Zhang, W. Finite-time chaos synchronization of unified chaotic system with uncertain parameters. *Commun. Nonlinear Sci. Numer. Simulat.* **2009**, *14*, 2239–2247. [[CrossRef](#)]
24. Almatroud, A.O. Synchronisation of two different uncertain fractional-order chaotic systems with unknown parameters using a modified adaptive sliding-mode controller. *Adv. Differ. Equations* **2020**, *2020*, 1–14. [[CrossRef](#)]
25. Heidarzadeh, S.; Shahmoradi, S.; Shahrokhi, M. Adaptive synchronization of two different uncertain chaotic systems with unknown dead-zone input nonlinearities. *J. Vib. Control.* **2020**, *26*, 1956–1968. [[CrossRef](#)]
26. Li, J.; Qian, C. Global Finite-Time Stabilization by Dynamic Output Feedback for a Class of Continuous Nonlinear Systems. *Trans. Autom. Control.* **2006**, *51*, 879–884. [[CrossRef](#)]
27. Zhou, S.; Hong, Y.; Yang, Y.; Lü, L.; Li, C. Finite-time synchronisation of uncertain delay spatiotemporal networks via unidirectional coupling technology. *Pramana* **2020**, *94*, 1–10. [[CrossRef](#)]
28. Slotine, J.; Li, W. *Applied Nonlinear Control*; Prentice-Hall: Englewood Cliffs, NJ, USA, 1991.
29. Yuan, C.; Ling, L.; Zhao, H. Lag synchronization between discrete chaotic systems with diverse structure. *Appl. Math. Mech.* **2010**, *31*, 733–738.
30. Jian-Fen, L.; Hui, L.; Nong, L. Chaotic synchronization with diverse structures based on tracking control. *Acta Phys. Sin.* **2006**, *55*, 3992–3996.

31. Zheng, Q.; Zhang, X.; Ren, Z. Anti-synchronization between Lorenz and Liu between Lorenz and Liu hyperchaotic systems. *Commun. Theor. Phys.* **2008**, *50*, 677–680.
32. Wang, Z.; Shi, X. Anti-synchronization of Liu system and Lorenz system with known or unknown parameters. *Nonlinear Dyn.* **2009**, *5*, 425–430. [[CrossRef](#)]

Publisher’s Note: MDPI stays neutral with regard to jurisdictional claims in published maps and institutional affiliations.



© 2020 by the authors. Licensee MDPI, Basel, Switzerland. This article is an open access article distributed under the terms and conditions of the Creative Commons Attribution (CC BY) license (<http://creativecommons.org/licenses/by/4.0/>).